



HAL
open science

Cognitive and hormonal regulation of appetite for food presented in the olfactory and visual modalities

R Janet, A Fournel, M Fouillen, E. Derrington, M Bensafi, Jean-Claude Dreher

► **To cite this version:**

R Janet, A Fournel, M Fouillen, E. Derrington, M Bensafi, et al.. Cognitive and hormonal regulation of appetite for food presented in the olfactory and visual modalities. *NeuroImage*, 2021, 117811. hal-02990722

HAL Id: hal-02990722

<https://hal.science/hal-02990722>

Submitted on 6 Nov 2020

HAL is a multi-disciplinary open access archive for the deposit and dissemination of scientific research documents, whether they are published or not. The documents may come from teaching and research institutions in France or abroad, or from public or private research centers.

L'archive ouverte pluridisciplinaire **HAL**, est destinée au dépôt et à la diffusion de documents scientifiques de niveau recherche, publiés ou non, émanant des établissements d'enseignement et de recherche français ou étrangers, des laboratoires publics ou privés.

1
2 **Cognitive regulation of multimodal food perception**
3 **in the human brain**
4
5
6
7

8 **R. Janet** ^{1,3}, **A. Fournel** ^{2,3}, **M. Fouillen** ^{1,3}, **E Derrington** ^{1,3}, **M Bensafi** ^{2,3}, **JC. Dreher** ^{1,3}
9

10
11
12 ¹ CNRS-Institut des Sciences Cognitives Marc Jeannerod, UMR5229, 'Neuroeconomics,
13 reward, and decision making laboratory', 67 Bd Pinel, 69675 Bron, FRANCE
14

15 ² Lyon Neuroscience Research Center, CNRS UMR5292, INSERM U1028, University of
16 Lyon, Lyon, FRANCE
17

18 ³ Univ Lyon, Université Claude Bernard Lyon 1, ISCMJ, F-69675, LYON, FRANCE
19

20 **Corresponding author:**

21 Dr Jean-Claude Dreher,
22 Research director, CNRS UMR 5229
23 Neuroeconomics group, Reward and decision making
24 Institut des Sciences Cognitives Marc Jeannerod,
25 67 Bd Pinel, 69675 Bron, France
26 tel: 00 334 37 91 12 38
27 fax: 00 334 37 91 12 10
28 <https://dreherteam.wixsite.com/neuroeconomics>
29

30 Manuscript information: 51 pages, 6 figures, 4 tables, 150 words in the abstract, 742 words
31 in the introduction and 1790 words in the discussion
32

33 **Declaration of Interests**

34 The other authors declare no conflict or no competing of interest.

35 **Acknowledgments.**

36 This work was performed within the framework of the Laboratory of Excellence LABEX ANR-
37 11-LABEX-0042 of Université de Lyon, within the program "Investissement d'Avenir" (ANR-
38 11-IDEX-0007) operated by the French National Research Agency (ANR). This work was also
39 supported by grants from the Agence Nationale pour la Recherche (ANR Social-POMDP). We
40 thank the staff of CERMEP–Imagerie du Vivant (Lyon) for helpful assistance with data
41 collection.
42
43

44 **The ability to regulate appetite is essential to avoid food over-consumption. The**
45 **desire for a particular food can be triggered by its odor before it is even seen.**
46 **Using fMRI, we identify the neural systems modulated by cognitive regulation**
47 **when experiencing appetizing food stimuli presented in both olfactory and**
48 **visual modalities, while being hungry. Regulatory instruction modulated bids**
49 **for food items and inhalation patterns. Distinct brain regions were observed for**
50 **up and down appetite-regulation, respectively the dorsomedial prefrontal cortex**
51 **(dmPFC) and dorsolateral PFC. Food valuation engaged the ventromedial PFC**
52 **and bilateral striatum while the amygdala was modulated by individual food**
53 **preferences, indexed by rank-ordered bids. Furthermore, we identified a**
54 **neurobiological marker for up-regulating success: individuals with higher blood**
55 **levels of ghrelin were better at exercising up-regulation, and engaged more the**
56 **dmPFC. This characterizes the neural circuitry regulating food consumption and**
57 **suggests potential hormonal and neurofunctional targets for preventing eating**
58 **disorders.**

59

60 **Keywords: food, regulation, fMRI, Ghrelin**

61 **Introduction**

62 Eating disorders such as binge eating disorder represent a public health
63 challenge because they are associated with high comorbidity and serious health
64 consequences (Hoek et al., 2016). The rising rates in obesity (Flegal et al., 2016;
65 Gallus et al., 2015; Sturm et al., 2013) also emphasize the crucial need to understand
66 the neurocomputational mechanisms underlying the regulation of food consumption,
67 especially in a context of overexposure to food stimuli. Food consumption may be
68 regulated through the implementation of strategies, known as cognitive regulation.
69 These strategies use attention, language and executive control to modulate the value
70 people attribute to features of visual stimuli (Adcock et al., 2006; Galsworthy-Francis
71 and Allan, 2014; Yokum and Stice, 2013). Cognitive regulation thus serves as an
72 important strategy by which the brain can control food craving.

73 Most of our knowledge about the neurobiological mechanisms underlying
74 cognitive regulation of food stimuli is derived from fMRI studies using food images only
75 (Hutcherson et al., 2012; Inui et al., 2004; Kober et al., 2010). These studies reported
76 that presentation of visual food-cues engages brain regions associated with reward
77 and valuation, the bilateral striatum and the ventromedial prefrontal cortex.
78 Accumulated evidence indicate that the lateral prefrontal cortex (IPFC) also plays a
79 key role in modulating food cue induced signals by the use of cognitive strategies
80 (Hollmann et al., 2012; Hutcherson et al., 2012b; Kober et al., 2010; Siep et al., 2012a;
81 Yokum and Stice, 2013 Schmidt et al., 2018). Early studies reported that the IPFC,
82 supporting cognitive regulation, acts on value signals encoded in the ventromedial
83 PFC (vmPFC) (Hare et al., 2009; Kober et al., 2010, Hutcherson et al., 2012b).
84 However, a recent study found that the vmPFC activity may be insensitive to
85 regulatory goals during cognitive regulation (Tusche and Hutcherson, 2018),

86 suggesting that cognitive regulation acts upstream of the integrated value signal by
87 modulating specific attributes value (Inzlicht et al., 2016).

88 Yet, little is known about the neurobiological mechanisms underlying appetite
89 regulation of food stimuli presented in a more realistic and ecological fashion, such as
90 when combining visual cues with food odors. Food odors are potent signals for
91 triggering appetite. For example, the smell of a croissant wafting from a patisserie, can
92 trigger a strong desire for this food in the absence of any visual cue. Parallels may
93 exist between the neural mechanisms engaged in cognitive strategies used for
94 emotion regulation and for the regulation of appetite (Buhle et al., 2014; Kober et al.,
95 2010). Both types of regulatory mechanisms may engage common brain regions, such
96 as the dorsolateral PFC (dlPFC) for down-regulation (Frank et al., 2014) and the
97 anterior medial part of the PFC for up-regulation (Ochsner et al., 2004). We therefore
98 hypothesized that the lateral PFC may play a role in down-regulating food craving
99 whereas the medial part of the PFC may support up-regulation of appetite.

100 Furthermore, homeostatic peptide hormones such as ghrelin, produced in the
101 gastrointestinal tract and leptin, produced in adipose cells and the small intestine,
102 convey energy balance information to the brain that affect food intake. Ghrelin acts
103 both on the homeostatic hypothalamic-brainstem circuits regulating energy balance
104 and on systems involved in reward and motivation (Mason et al., 2013; Perello and
105 Dickson, 2015). High levels of ghrelin, either due to ghrelin injection or fasting,
106 increase motivation for food rewards and modulate the reward system (Abizaid et al.,
107 2006; Han et al., 2018; Karra et al., 2013; Kroemer et al., 2013; Shirazi et al., 2013).
108 However, it remains unknown whether ghrelin modulates the brain systems engaged
109 in appetite up-regulation in humans.

110 Here, we used fMRI to investigate the neural processes involved in appetite
111 regulation during successive presentation of food odor and image. Healthy hungry
112 participants made real food purchase decisions under a Natural control condition and
113 two cognitive regulation conditions after smelling a food odor paired with a
114 corresponding food picture. We investigated: 1) whether cognitive regulation
115 modulates sniffing and subjective preferences for food, as assessed by willingness to
116 pay; 2) which brain areas support valuation of food cues presented sequentially in the
117 olfactory and visual modalities; 3) whether distinct or common PFC areas support up-
118 and down-regulation of salient food items; 4) whether brain regions involved in the
119 valuation of food cues are functionally modulated by regulatory regions; 5) whether
120 individual preferences for specific odors have a specific neural signature (by rank
121 ordering each food category according to each participants' preferences); 6) what are
122 the contributions of ghrelin and leptin to appetite regulation under cognitive regulation.

123 Results

124 Behavior

125 Prior to scanning, participants rated their appetite on a continuous scale
126 (ranging from “0”= not hungry at all, 50= moderately hungry; to “100”= never been so
127 hungry). The food quantity participants would be willing to eat prior to scanning was
128 also assessed on a similar continuous scale. Participants rated their appetite at 60.4%
129 (SEM= 4.7) and their food quantity at 75.1 (SEM= 3.2). This procedure allowed us to
130 ensure that participants felt subjectively hungry and were willing to eat a large quantity
131 of food. We also found a positive correlation between participants’ appetite and their
132 blood level of ghrelin ($r=0.495$, $p=0.016$) and a positive trend between blood level of
133 ghrelin and the quantity of food participants were willing to eat ($r=0.406$, $p =0.054$).

134 We found that cognitive regulation had a significant effect on average bidding
135 behavior ($F_{(2,46)} = 240.951$, $p<0.001$) (Figure 2A). *Post hoc* analysis revealed that,
136 compared to the Natural condition (the no cognitive regulation condition) (mean (M)
137 $1.52 \pm$ (SEM) 0.011), participants bid significantly more under the Indulge (the positive
138 cognitive regulation condition) ((M) $2.03 \pm$ (SEM) 0.011 ; paired $t_{(24)} = 12.508$ $p<0.001$)
139 and less under the Distance condition (the negative cognitive regulation condition)
140 ((M) $0.871 \pm$ (SEM) 0.007 ; paired $t_{(24)} = 11.197$ $p<0.001$) (paired t-test with Bonferroni
141 correction). We also controlled for possible interactions between regulatory conditions
142 and food odor category (Apricot, Pineapple, Milk Chocolate or Dark Chocolate). This
143 analysis revealed no significant interaction between cognitive regulation and types of
144 food odor categories ($F_{(3,72)} = 0.934$, $p=0.469$). This analysis also revealed that
145 participants’ bids differed according to the food category ($F_{(3,72)} = 118.079$, $p<0.001$)
146 (Figure 2B). *Post-hoc* tests revealed that participants bid less for Pineapple ((M) 1.32
147 \pm (SEM) 0.016) compared to milk chocolate ((M) $1.32 \pm$ (SEM) 0.016) ($p < 0.005$,

148 paired $t_{(24)} = -3.145$) and compared to dark chocolate ((M) $1.32 \pm$ (SEM) 0.016) ($p <$
149 0.05 , paired $t_{(24)} = -2.789$).

150 Reaction Times (RTs) also differed between conditions ($F_{(2,46)} = 16.247$,
151 $p < 0.001$) (Figure 2C). Participants' bids were faster in the Indulge condition ((M) 1.50
152 \pm (SEM) 0.015) compared to the Natural ((M) $1.90 \pm$ (SEM) 0.024 ; paired $t_{(24)} = 5.825$
153 $p < 0.001$) and Distance conditions ((M) $1.95 \pm$ (SEM) 0.025) (paired $t_{(24)} = 5.221$
154 $p < 0.001$).

155

156 Olfactomotor responses (sniffing)

157 A significant effect of regulatory instructions was observed on the duration of
158 the first sniff (Friedman test, $\chi^2_{(3)} = 30.064$, $p = 0.001$) (Figure 2D, Duration of first
159 sniff). There was a significant decrease in the duration of sniffing in the Distance ((M)
160 $1.86 \pm$ (SEM) 0.015) compared to the Natural condition ((M) $1.94 \pm$ (SEM) 0.016) (p
161 $= 0.011$, paired $t_{(24)} = -2.92$). Participants inhaled for a shorter period during the Air-
162 clean ((M) $1.76 \pm$ (SEM) 0.012) condition compared to the Distance, Indulge ((M) 1.95
163 \pm (SEM) 0.016) and Natural conditions. No significant difference in sniffing duration
164 was found between the Indulge and Natural conditions (paired $t_{(24)} = 2.587$, $p =$
165 0.096).

166 A significant effect of regulatory instructions was observed concerning the
167 amplitude of the first sniff ($F_{(3,72)} = 4.248$, $p = 0.008$) (Figure 2E, Amplitude of first
168 sniff). A *post-hoc* test with the Bonferroni correction showed a significant decrease in
169 the amplitude of sniffing in the Distance ((M) $2.47 \pm$ (SEM) 0.035) compared to the
170 Indulge condition ((M) $2.61 \pm$ (SEM) 0.033) ($p = 0.025$, paired $t_{(24)} = -3.139$). No
171 significant effect of condition was observed on the volume of the first sniff ($F_{(3,72)} =$
172 2.587 , $p = 0.06$).

173 We next considered the entire sniffing period during odor presentation. We
174 found a significant difference between conditions with respect to the total number of
175 sniffing cycles ($F_{(3,72)} = 3.962, p = 0.011$) (Figure 2F, Mean sniff number). *Post-hoc*
176 analysis revealed that participants had more sniffing cycles in the Natural condition
177 compared to the Air-clean condition ($p = 0.024, \text{paired } t_{(24)} = -2.65$).

178 A significant effect of conditions was observed on the average sniffing
179 amplitude during the total sniffing period ($F_{(3,92)} = 6.068, p = 0.001$) (Figure 2G, cycle
180 amplitude). A *post-hoc* test with Bonferroni correction showed a significant increase in
181 the average amplitude of sniffing in the Indulge ((M) $2.45 \pm (\text{SEM}) 0.035$) compared to
182 the Natural conditions ((M) $2.34 \pm (\text{SEM}) 0.035$) ($p = 0.037, \text{paired } t_{(24)} = -2.448$). The
183 *Post-hoc* test also revealed a significant increase in the amplitude of sniffing in the
184 Indulge compared to the Air-clean conditions ((M) $2.35 \pm (\text{SEM}) 0.034$) ($p = 0.011,$
185 $\text{paired } t_{(24)} = -2.346$). Finally, no significant difference concerning the sniffing
186 amplitude was observed between the Indulge and Distance conditions.

187 A significant effect of conditions was observed on the average sniff volume
188 during the total sniffing period ($F_{(3,72)} = 7.863, p = 0.001$) (Figure 2H, Mean sniff
189 volume). A *post-hoc* test with the Bonferroni correction showed a significant increase
190 in the mean volume of sniffing in the Indulge ((M) $2.41 \pm (\text{SEM}) 0.037$) compared to
191 the Natural condition ((M) $2.26 \pm (\text{SEM}) 0.036$) ($p = 0.028, \text{paired } t_{(24)} = -2.448$). They
192 also revealed an increase in the average volume of sniffing in the Indulge compared
193 to Distance conditions ((M) $2.22 \pm (\text{SEM}) 0.036$). Finally, the *post-hoc* test also
194 revealed a significant increase in the average volume of sniffing in the Indulge
195 condition compared to the Air-clean trials ((M) $2.20 \pm (\text{SEM}) 0.036$) ($p = 0.004, \text{paired}$
196 $t_{(24)} = -2.346$).

197 No significant effect of conditions was observed concerning the mean duration
198 of sniffing during the entire period of odor presentation ($F_{(3,72)} = 1.313, p = 0.277$).

199 We also investigated potential differences between men and women in their
200 capability to regulate their appetite. Using a Two-way ANOVA, we found no significant
201 difference between sex concerning bid ($F_{(5,120)} = 4.229, p = 0.132$) or RTs ($F_{(5,120)} =$
202 $5.603, p = 0.099$). When performing the same analysis on breathing parameters, we
203 observed no significant differences for the volume ($F_{(7,168)} = 0.014; p = 0.907$),
204 amplitude ($F_{(7,168)} = 1.31; p = 0.282$) and the duration of the first sniff ($F_{(7,168)} = 4.42;$
205 $p = 0.065$). Despite the fact that men have a greater total lung capacity (LoMauro and
206 Aliverti, 2018) we found no differences between men and women in breathing
207 parameters.

208

209 **fMRI results**

210 *Neurocomputational mechanisms of cognitive regulation of food*

211 First, using the GLM1, we searched for brain regions engaged in cognitive
212 regulation during the odor/image presentation. As shown in Figure 3, Table 1, when
213 averaging over the period of odor/image presentation, BOLD response in the
214 dorsomedial PFC was significantly higher in the Indulge compared to Natural condition
215 (comparison Indulge > Natural) ($x, y, z: -4, 58, 21; t = 5.43; p < 0.05$ Family-Wise Error
216 (FWE) whole brain cluster corrected). To illustrate the response in this brain region,
217 we extracted beta parameters in the three different conditions and plotted them (Bar
218 Graphs). We also investigated the opposite contrast (Natural > Indulge). No brain
219 region showed greater activity under Natural trials compared to Indulge trials.

220 Comparison of the Distance condition with the Natural condition (Distance >
221 Natural) revealed a significant increase of the BOLD signal in the bilateral superior

222 PFC (x,y,z: -24, 52, 22; 20, 46, 30; t = 6.76 and 4.94 for Left and Right respectively),
223 the right dIPFC (x,y,z: 44, 16, 46; t = 5.35), the anterior cingulate cortex/supplementary
224 motor area (ACC/SMA) (x,y,z: 3, 8, 62; t = 5.20) and bilateral angular gyrus (x,y,z: 56,
225 -54, 27; -46, -60, 39; t = 4.22 and t = 4.13 for right and left respectively) ($p < 0.05$ FWE
226 whole brain cluster corrected) (Figure 4, Table 1). Again, we also plotted the beta
227 parameters from these regions in the three different conditions (Figure 4). Finally,
228 investigation of the contrast (Natural > Distance) revealed no brain region showing
229 greater activity in Natural trials as compared to Distance trials.

230

231 *Relationships between Ghrelin/leptin levels and brain activity related to different*
232 *regulatory conditions*

233 Because up-regulation during the Indulge condition selectively increased
234 activity in the dorsomedial dmPFC, we thought to investigate the link between this
235 brain response and leptin/ghrelin levels. To determine the potential relationship
236 between hormone levels and regulatory mechanisms, we conducted a correlation
237 analysis between the beta extracted from the dmPFC ROI (8 mm sphere centered on
238 the peak dmPFC cluster identified in the comparisons Indulge>Natural) and
239 leptin/ghrelin levels. We observed a positive correlation between total ghrelin and
240 betas extracted from the dmPFC ROI in the Indulge ($r = 0.469$, $p = 0.024$) and between
241 ghrelin and betas in the Natural condition ($r = 0.511$, $p = 0.013$). No significant
242 correlation was found between beta parameters from regions revealed by the contrast
243 Distance > Natural and ghrelin level (Figure. 3B). The same procedure was conducted
244 for leptin level but no significant correlations were revealed. Finally, we defined the
245 'regulatory success of Willingness To Pay' (WTP) as the WTP difference between the
246 Indulge and Natural conditions for a given food (represented by an odor followed by a

247 picture) in each case where participants bid more in the Indulge condition compared
248 to Natural condition. The same procedure was used to compute the absolute value of
249 the difference in WTP between Distance and Natural conditions for the cases where
250 participants bid less in the Distance condition than in the Natural condition. We then
251 conducted Pearson correlation analysis to determine if the ghrelin level is correlated
252 with regulatory success when up- or down regulating. We observed a significant
253 correlation between ghrelin levels and up-regulation ($r= 0.373$; $p = 0.002$) but not
254 between ghrelin levels and down-regulation ($p = 0,516$) (Figure 3C).

255

256 *Subjective value computation at the time of Willingness to Pay*

257 Next, we searched for brain areas engaged in odor/image value computation
258 using GLM2. We found that the vmPFC (x,y,z: 6, 42, 3; $t = 3.96$), and bilateral VSTR
259 (x,y,z: -6, 14, -4; $t = 4.20$ and 6, 18, -2; $t = 3.62$ respectively left and right) positively
260 correlated with participants' bid in the Natural condition ($p<0.05$, FWE corrected within
261 small volume correction) (Figure. 5, Table 2). Note that we used Natural trials only to
262 determine brain areas correlating with WTP because there was not enough variation
263 in the bids in the Indulge and Distance conditions to perform regression analyses
264 between WTP and the BOLD signal. Indeed, WTP were always high in the Indulge
265 condition and always low in the Distance condition, relative to the Natural condition.
266 This prevented us to observe value signals across all conditions and to test for
267 changes in slopes between value representation (as indexed by brain regressions with
268 WTP) and regulatory conditions. Thus, we defined ROIs to investigate whether
269 regulatory instructions modulated activity in the vmPFC and bilateral striatum. That is,
270 we defined vmPFC and bilateral VSTR as spherical ROIs based on previous analyses
271 reporting these regions as key areas for valuation (Clithero and Rangel, 2013;

272 Hutcherson et al., 2012; Kober and Mell, 2015; Metereau and Dreher, 2015; Todd A.
273 Hare, Colin F. Camerer, 2007) Within these ROIs, we used GLM1 to search for
274 significant differences between regulatory instructions. The results revealed no
275 significant differences across conditions within these ROIs. To illustrate this, we
276 extracted beta parameters from these ROIs in the three different conditions and plotted
277 them (Figure 5).

278

279 *Neural representations of individual odor ranking*

280 To test for brain regions involved in the individual ranking preferences of food
281 categories, we used GLM3 (see methods) classifying food categories for each
282 participant from the most preferred to the least preferred food category, based on
283 mean bid, regardless of condition. Re-ranking each odor from the least preferred odor
284 (R2) to the most preferred odor (R5) for each individual subject, we then tested for
285 individual processing of food categories using linear combination: R2; R3; R4 and R5,
286 and then used a regression test $R2 < R3 < R4 < R5$ at the group level to identify brain
287 regions encoding individual ranking preferences of food during the odor presentation.
288 This analysis revealed that the right amygdala (x,y,z: 24, 2, -20; $t = 4.76$), and bilateral
289 occipital cortices (x,y,z: -24, -96, -12 / 22, -93, -9) correlated robustly and positively
290 with food ranking preferences at the time of odor presentation (Figure 6, Table 3,
291 $p < 0.05$ FWE whole brain peak cluster corrected). The left amygdala was also found to
292 be engaged in this correlation at a lower threshold ($p < 0.005$, uncorrected).

293 To test for any effect of conditions-by-preferences interaction we used a flexible
294 factorial design including regressors denoting individual ranking preferences per
295 condition during odor presentation. No significant BOLD response was observed in

296 any brain areas supporting individual ranking preferences (Table 3, $p < 0.05$ FWE
297 whole brain cluster corrected).

298

299 *Functional connectivity analysis*

300 To test for changing functional connectivity according to regulation conditions
301 between brain regions engaged in cognitive regulation (i.e. dlPFC and dmPFC
302 identified with the GLM1) and a core component of the valuation network, i.e. the
303 vmPFC, we performed a generalized PsychoPhysiological Interaction (gPPI) using the
304 CONN toolbox. A gPPI model allows us to explore the physiological response (HRF
305 convolved BOLD signal) in one region of the brain in terms of the context-dependent
306 response of another region. This effectively provides a measure of task-modulated
307 connectivity between two or more regions. Here, we conducted two ROI-to-ROI gPPI
308 analysis using the CONN Toolbox (www.nitrc.org/projects/conn, RRID:SCR_009550).
309 The first analysis was performed to investigate the functional connectivity between the
310 dmPFC and the vmPFC during the Indulge compared to the Natural conditions, taking
311 the dmPFC as a seed region (gPPI-1). The second analysis investigated the functional
312 connectivity between the bilateral superior PFC, the dlPFC and the vmPFC during the
313 Distance compared to the Natural conditions (gPPI-2).

314 The results revealed no significant differences in functional connectivity
315 between the cognitive regulation brain regions identified using the GLM1 and the
316 vmPFC during the perception of the combined olfacto-visual stimuli during the Indulge
317 regulation compare to the Natural condition (Table 4). They neither revealed significant
318 differences in functional connectivity between the right dlPFC or bilateral superior PFC
319 and the vmPFC during the Distance condition compared to the Natural condition (peak

320 voxel-level at $p < 0.001$, corrected at the cluster-level using a family-wise error rate
321 (FDR) of $p < 0.05$ two-sided) (Table 4).

322

323 **Discussion**

324 One important aspect of this study was to investigate, in food deprived
325 participants, the neural mechanisms engaged in cognitive regulation of food stimuli
326 presented in the visual and olfactory domains. Both willingness to pay for food and
327 sniffing parameters were modulated by regulatory conditions, indicating reliable
328 regulatory mechanisms at the behavioral and physiological levels. At the brain system
329 level, increased dorsomedial PFC activity occurred during up-regulation of appetite
330 (Figure 3A), whereas a brain network, including the bilateral IPFC, the right dlPFC and
331 the ACC was more engaged during down-regulation of appetite as compared to the
332 Natural condition (Figure 4). Activity from to the valuation system, including the vmPFC
333 and bilateral striatum correlated with increasing WTP assigned to the food, but was
334 not modulated by appetite regulatory instructions, confirming that engagement of this
335 brain system is relatively automatic (Figure 5). Finally, the amygdala response
336 positively correlated with the individual preference for the specific food presented, and
337 this 'odor-specific preference' response was also resilient to neuroregulatory
338 instructions. Together, these results demonstrate the existence of separate brain
339 systems responding or not to appetite regulation when subjects are hungry.

340 Our findings provide novel insights into the neurobiological mechanisms
341 involved in the cognitive regulation of ecological bimodal food cues. First, cognitive
342 regulation modulated the duration (Figure 2D) and the amplitude (Figure 2E) of the
343 first inspiration, showing that physiological parameters of the olfactory system are
344 under modulation of cognitive regulation. Our results extend early findings on cognitive
345 regulatory mechanisms, and highlight the fact that human sniffing is influenced by
346 internal states, such as motivation or homeostatic state. For example, hunger
347 increases sniff duration compared to satiety, even when sniffing clean air (Prescott et

348 al., 2010). Cognitive regulation also modulated parameters of the entire sniffing period
349 (Figures 2H, 2G). These results suggest that cognitive regulation can control sniff
350 parameters and modulate behavior. This is consistent with the fact that breathing
351 phase modulates discrimination of fearful faces, as fearful faces were recognized more
352 quickly during expiration compared to inspiration (Zelano et al., 2016). Together, these
353 inhalation results suggest that subjects have meta-cognition about the impact of odors
354 in their self-control, and that they try to influence their regulatory abilities by accessing
355 this mechanism. This is an important finding because much remains to be learnt about
356 the channels through which individuals exercise dietary control. Finally, participants'
357 WTP for food was higher in the Indulge condition, as compared to the Natural
358 condition, whereas they bid less under the Distance condition (Figure 2A). These
359 findings extend previous results restricted to the visual modality to multimodal food
360 stimuli (Boswell et al., 2018; Hutcherson et al., 2012) and further show that humans
361 are able to regulate their WTP when the food is presented in both olfactory and visual
362 modalities.

363 The increased engagement of the dorsomedial PFC (dmPFC) observed with
364 up-regulation of appetite towards food stimuli is consistent with the fact that this brain
365 region shows a specific heightened response to food when subjects are hungry
366 (Anderson et al., 2006; Giannopoulou et al., 2018; LaBar et al., 2001) (Figure 3A). This
367 finding supports the idea that this brain region modulates motivation towards food.
368 These results suggest that during up-regulation, activity within the dmPFC increases
369 together with a concurrent increase in appetite towards food stimuli. In obese
370 populations, a meta-analysis revealed higher activity of the dmPFC when viewing food
371 pictures (Brooks et al., 2013) while patients suffering from Binge Eating Disorders rate
372 food stimuli as significantly less desirable than healthy controls (Uher et al., 2004).

373 Conversely, the dlPFC, bilateral superior PFC and the ACC were more active
374 when participants down-regulated their appetite towards food odor/image stimuli
375 (Figure 4). The dlPFC is known to be engaged in regulation of appetite for visually
376 presented food stimuli (Hutcherson et al., 2012a; Kober et al., 2010; Lewis and Bates,
377 2014, Tusche and Hutcherson, 2018) and the ACC plays a critical role in response
378 inhibition and in the selection of appropriate behavior to resolve situations such as
379 action suppression (Cole and Schneider, 2007; Simmonds et al., 2008). Moreover, the
380 bilateral superior PFC has been associated with cognitive strategies to suppress the
381 desire for food stimuli (Siep et al., 2012b). Engagement of a brain network including
382 the dlPFC has been reported in emotional down-regulation of odors (Billot et al., 2017).
383 Moreover, regulation-related neural activation patterns in a right dlPFC area has been
384 shown to reliably predict how well participants decrease taste weights attribute in food
385 choices (Tusche et al., 2018). Together, these findings are consistent with the
386 hypothesis that cognitive regulation of appetite and emotional regulation may share
387 common neural substrates because increased dlPFC response has been observed
388 during down-regulation of negative emotion, and decreased dlPFC activity has been
389 found during down-regulation of positive emotion (Ochsner and Gross, 2005).

390 When investigating the brain systems engaged in the valuation of food items in
391 response to ecological cues in the absence of cognitive regulation (Natural condition),
392 we observed engagement of the valuation brain system, consisting of the vmPFC and
393 the bilateral striatum (Figure 5). These brain regions have previously been shown to
394 be key for valuation of food items presented visually (Clithero and Rangel, 2013). We
395 extend these previous results to multimodal situations in which food is experienced in
396 the visual and olfactory modalities. Such vmPFC engagement in the valuation of a
397 food item is much closer to experiencing real food (combining vision, smell and taste).

398 This brain region has also been observed during anticipation of salient food (liquid)
399 reinforcers that are really delivered inside the scanner (Metereau and Dreher, 2015;
400 O'Doherty et al., 2002). Thus, vision and smell play a key role in constructing a unified
401 and co-occurring percept defined as flavor when anticipating and experiencing food
402 items.

403 It should be noted that none of the brain valuation regions were modulated by
404 cognitive regulation. In fact, distinct brain regions were engaged during the Indulge
405 and Distance conditions. This confirms that valuation is relatively automatic, as
406 previously suggested (Lebreton et al., 2009) and that cognitive regulation of food odor
407 and image does not modulate the valuation system itself. A number of previous studies
408 using similar paradigms but only with food presented in the visual domain (Hare et al.,
409 2009, 2011; Hutcherson et al., 2012; Krishna, 2012), have reported that regulation
410 involves the modulation of value signals in the vmPFC, as well as interaction with
411 regions like the dlPFC. To investigate whether this was the case in the current dataset,
412 we performed a functional connectivity analysis between the regions engaged in
413 cognitive regulation and the vmPFC. Using ROI-to-ROI gPPI analysis, we
414 investigated changes in connectivity pattern between the dmPFC and the vmPFC
415 during the Indulge as compared to the Natural conditions. We also investigated
416 changes in connectivity patterns between the right dlPFC, the bilateral superior IPFC
417 and the vmPFC during the Distance as compared to the Natural conditions. These
418 analyses failed to reveal that cognitive regulation is exerted by changed in functional
419 connectivity between the dmPFC and the vmPFC during the Indulge vs Natural
420 conditions. No functional change in connectivity was observed between the dlPFC or
421 bilateral superior IPFC and vmPFC for the Distance vs Natural conditions either (see
422 results section and Table 4). Although these findings may be surprising at first stake,

423 a number of previous failures to observe changes in modulation of the vmPFC during
424 cognitive regulation of decision making suggest an alternative hypothesis (Hollmann
425 et al., 2012; Yokum and Stice, 2013; Tusche et al., 2018). It is possible that in our
426 study, as in these previous studies, cognitive regulation alters value representations
427 at a relatively low level, by amplifying or diminishing attribute representations directly
428 in a distributed set of specific, dedicated attribute-coding areas. Consistent with this
429 possibility, a recent study observed that cognitive regulation did not operate at higher
430 levels in centralized, domain-general value integration area such as the vmPFC
431 (Tusche and Hutcherson, 2018). Instead, cognitive regulation of decision-making
432 altered value representations at a relatively low level, representing food attributes in a
433 dlPFC region. Further work will be needed to understand the respective roles of the
434 vmPFC and dlPFC, as well as their interactions during cognitive regulation of food
435 stimuli presented in multimodal domains.

436 Investigation of the brain regions encoding individual odor preferences, based
437 on rank ordering of the foods presented, showed that activity of the amygdala robustly
438 increased as a function of increasing odor preference (Figure 6). The cognitive
439 regulation conditions did not modulate this amygdala response, and there was also no
440 interaction between regulatory instruction and odor ranking at the behavioral level.
441 This amygdala response may thus correspond to a relatively automatic route that
442 integrates information about potential outcome value and action-outcome association
443 to guide choice behavior (Balleine and Killcross, 2006; O'Doherty, 2004; Saez et al.,
444 2017; Seymour and Dolan, 2008). Consistent with this interpretation, a previous study
445 showed that the amygdala encodes subjective valence of odors (Jin et al., 2015).

446 Finally, correlational analysis revealed a positive relationship between blood
447 levels of ghrelin and BOLD response in the dmPFC that up-regulated the subjective

448 value of food items in the Indulge condition (Figure 3B). Individuals with higher blood
449 levels of ghrelin were better at exercising up-regulation as they showed higher up
450 regulatory success when comparing bids from the Indulge vs Natural conditions
451 (Figure 3C). Thus, the relationship between dmPFC activity and ghrelin levels may be
452 a neurobiological marker for up-regulation success. Ghrelin regulates food intake
453 (Date et al., 2001; Müller et al., 2015) and levels of ghrelin positively correlate with
454 increased hunger and with increasing activity in large brain networks involved in the
455 regulation of feeding and in the appetitive response to food cues (Batterham et al.,
456 2007; Goldstone et al., 2004; Jones et al., 2012; Wei et al., 2015; Zanchi et al., 2017).
457 All these studies showed increased neural response to food pictures in regions of the
458 brain engaged in encoding the automatic incentive value of food cues, but did not
459 investigate how ghrelin modulates brain regions engaged with up-regulation of food
460 cues, as in the current study. Ghrelin may act on the brain through several
461 mechanisms, including ghrelin receptors in the gut relaying information *via* the vagus
462 nerve (Date, 2013), the hypothalamus regulating feeding behavior and the
463 dopaminergic system (Abizaid et al., 2006; Perello et al., 2012). Our results suggest
464 that the dmPFC plays a crucial role in the relationship between ghrelin and up-
465 regulation of feeding behavior.

466 Together, our results demonstrate that in the context of hunger, up- and down-
467 regulation of appetite towards realistic food stimuli presented in the olfactory and visual
468 domains are mediated by distinct brain networks. The medial prefrontal cortex is
469 engaged in up-regulation whereas the lateral prefrontal cortex is engaged in down-
470 regulation. Our findings also provide new insights to the relationship between higher-
471 level brain regions engaged in up-regulating food consumption and ghrelin.

472

473 **Materials and Methods**

474 **Participants**

475 Twenty five healthy volunteers (12 females, 13 males; age range 18-33 years;
476 and mean age (M) $22.45 \pm$ (SEM) 3.88) were recruited through a mailing list from the
477 University of Claude Bernard Lyon 1. All participants had a normal Body Mass Index
478 (BMI) (mean (M) $21.74 \pm$ (SEM) 0.36). For inclusion in the study, participants were
479 required to follow the following criteria: french-speaking, right-handed, no current
480 medical treatment, no history of neurological or psychiatric disorders and no auditory,
481 olfactory or visual deficits. Furthermore, volunteers were screened for general MRI
482 contra-indications. A physician conducted medical examinations concerning inclusion
483 criteria such as physical and psychological health. Participants gave their written
484 consent and received monetary compensation for the completion of the study. This
485 study was approved by the Medical Ethics Committee (CPP Sud-Est III, ID RCD: 2014-
486 A011661-46).

487

488 **Stimuli and delivery**

489 Olfactory stimuli (apricot, pineapple, dark chocolate, milk chocolate, all
490 EURACLI products, Chasse-sur-Rhone, France; Respective concentration vol/vol:
491 75%, 25%, 75%, 75%) and corresponding visual stimuli (depicting desserts; 8 different
492 images *per* odor type (Figure 1B) were presented using a device adapted for fMRI
493 olfactory/visual experiments and described in details in Sezille et al. (Sezille et al.,
494 2013). Airflow control, odor concentration and stimulus duration, as well as collection
495 of participants' responses were all managed by the system, which is composed of a
496 series of modules: 1/ an airflow source, 2/ a diffusion module controlling odorant
497 duration and concentration through regulation of airflow, 3/ a mixing head used to (*i*)

498 mix non-odorized air from the first module with a specific odorant (controlled by the
499 second module) and (ii) send the diluted odor to the nose, 4/ a software enabling
500 presentation of verbal material (instructions) and visual stimuli, 5/ a response box to
501 provide subjective ratings.

502 To ensure synchronization between fMRI measures and odor diffusion,
503 olfactory stimuli were diffused at the beginning of each nasal inspiration. To this end,
504 the respiratory signal was acquired using an airflow sensor that was integrated with
505 an amplifier interface. A microbridge mass airflow (AWM2100V, Honeywell, MN, USA)
506 allowed acquisition of both inhalation and exhalation phases. The airflow sensor was
507 connected to a nasal cannula (Cardinal Health, OH, USA; 2.8 mm inner diameter tube)
508 positioned in both nostrils. Sniffing was digitally recorded at 100 Hz and stored in the
509 odor diffusion computer. Sniffs were pre-processed by removing baseline offsets, and
510 aligned in time by setting the point when the sniff entered the inspiratory phase as time
511 zero. Inspired volume, max amplitude rate and sniff durations were calculated for the
512 first sniff of every trial. Mean sniffing parameters during the entire odor presentation
513 was also recorded.

514 The whole system was controlled using LabVIEW® software. A multiple
515 function board (National Instruments, TX, USA) was used to acquire all experimental
516 events (olfactory, visual, instructions), signals from the respiratory sensor and the
517 response box, which allowed synchronization with the external system (fMRI scanner).

518

519 **Experimental design**

520 Each trial started with a visual instruction indicating the type of trial (i.e., Indulge,
521 Distance or Natural) for 3 s (seconds) (Figure 1A), followed by the diffusion of one of
522 the four categories of odors (apricot, pineapple, dark chocolate or milk chocolate) for

523 3.2 ± 0.8s, and synchronized with the respiration of the participants. Afterwards, a
524 visual image corresponding to the odor was presented for 2 s (e.g. a visual picture of
525 a pineapple pie following the smell of pineapple) (Figure 1B). Finally, the participants
526 had 5 s to select the price they were willing to pay for the presented food. Participants
527 were able to choose one price from the five depicted on the screen (i.e. € 0.50, € 1.00,
528 € 1.50 €2.00 or € 2.50); consistent with auction rules described by Becker-DeGroot-
529 Marschack (BDM) (M. Becker, Morris H. DeGroot, 1964; Plassmann et al., 2007).
530 Following participant's response, a fixation cross was presented for 5.4 ± 0.6s.

531 Before the "Modulatory instruction and bidding task" began, participants
532 received specific modulatory instructions for each trial type. For the Indulge condition,
533 participants were asked to smell the odor and to keep looking at the presented food
534 image while adopting thoughts that would increase their desire to eat the presented
535 food immediately. For the Distance condition, participants were asked to smell the
536 odor and keep looking at the presented food image while adopting thoughts that would
537 decrease their desire to eat the presented food immediately. For the Natural condition,
538 participants were asked to smell the odor and keep looking at the presented food
539 image while allowing any thoughts and feelings that came naturally in that moment.

540 Before scanning, participants were asked to rate how hungry they felt on a
541 continuous scale ranging from 0= "not hungry at all", 50 = "moderately hungry", to 100=
542 "never been so hungry". They also rated the quantity of food they were able to eat,
543 based on a similar continuous scale range from 0, "I cannot eat anything", to 100, "I
544 could eat anything". This allowed us to check the subjective hunger level of each
545 participant. The fMRI task consisted of 120 trials divided into four sessions. Each
546 session included 30 trials, 24 trials divided into the three trial types (i.e. 8 trials for each
547 condition) and six resting trials called Air-clean (i.e. in which no instruction, no odor

548 and no image were presented). Each session comprised a fixed order of presentation
549 of 30 trials. The four sessions were presented randomly to participants.

550 After scanning, blood samples were drawn by a nurse to later assess ghrelin
551 and Leptin levels.

552

553 **fMRI data acquisition**

554 All MRI acquisitions were performed on a 3 Tesla scanner using EPI BOLD
555 sequences and T1 sequences at high resolution. Scans were performed on a Siemens
556 Magnetom Prisma scanner HealthCare, CERMEP Bron (single-shot EPI, TR / TE =
557 2500/21, flip angle 80 °, 45 axial slices interlaced 2 mm thickness 2 mm gap, FOV =
558 232 mm and 116 die). A total of 1120 volumes were collected over four sessions during
559 the experiment, in an interleaved ascending manner. The first acquisition was done
560 after stabilization of the signal. Whole-brain high-resolution T1-weighted structural
561 scans (1 x 1 x 1 mm) were acquired for each subject, co-registered with their mean
562 EPI images and averaged across subjects to permit anatomical localization of
563 functional activations at the group level. Field map scans were acquired to obtain
564 magnetization values that were used to correct for field inhomogeneity.

565

566 **fMRI data preprocessing**

567 Image analysis was performed using SPM12 (Wellcome Department of Imaging
568 Neuroscience, Institute of Neurology, London, UK,
569 fil.ion.ucl.ac.uk/spm/software/spm12/). Time-series images were registered in a 3D
570 space to minimize any effect that could result from participant head-motion. Once
571 DICOMs were imported, functional scans were realigned to the first volume, corrected
572 for slice timing and unwarped to correct for geometric distortions. Inhomogeneous

573 distortions-related correction maps were created using the phase of non-EPI gradient
574 echo images measured at two echo times (5.40 ms for the first echo and 7.86 ms for
575 the second). Finally, in order to perform group and individual comparisons, they were
576 co-registered with structural maps and spatially normalized into the standard Montreal
577 Neurological Institute (MNI) atlas space. Following this, images were spatially
578 smoothed with an 8 mm isotropic full-width at half-maximum (FWHM) Gaussian kernel
579 using standard procedures in SPM12.

580

581 **fMRI data analysis and imaging statistics**

582

583 To address the questions raised in the introduction, that is whether: (1) cognitive
584 regulation modulates both sniffing and bidding behavior; 2) a common valuation
585 system is involved in the valuation of odor/image stimuli; 3) there are distinct brain
586 regions (especially prefrontal regions: dmPFC vs dlPFC) supporting up- and down-
587 regulation), we estimated three general linear models (GLMs). Each GLM was
588 estimated in three steps. First, we estimated the model separately for each individual.
589 Second, we calculated contrast statistics at the individual level. Third, we computed
590 second-level statistics by carrying out various statistical tests on the single-subject
591 contrast coefficients.

592 Statistical analyses were performed using a conventional two-level random-
593 effects approach with SPM12. All GLMs included the six motion parameters estimated
594 from the realignment step. Statistical inference was performed at a standard threshold
595 of $p < 0.05$, family-wise error (FWE) cluster-level corrected for multiple comparisons,
596 with an initial cluster-forming threshold of $p < 0.001$ and an extent $k = 40$ voxels.

597

598 *Analysis of cognitive regulation during odor/image presentation*

599 To determine the brain regions involved in cognitive regulation during the
600 odor/image presentation, we used GLM1. This GLM1 consisted of 9 regressors of
601 interest. Regressors R1–R3 modeled brain response related to the instructions
602 according to the condition, respectively Natural (R1), Indulge (R2) and Distance (R3).
603 R1-R3 were modeled as a boxcar function time-locked to the onset of the instruction
604 with duration of 3 s. R4 to R6 denoted regressors during food stimuli delivery in Natural
605 (R4), Indulge (R5) and Distance (R6) trials and were modeled as a boxcar function
606 beginning at odor presentation and during the entire period of food odor/image
607 presentation (mean 8.4 ± 1.6 s). Finally, R7 to R9 modeled brain response related to
608 the rating in the three regulatory instructions Natural (R7), Indulge (R8) and Distance
609 (R9). R7-R9 were modeled as a boxcar function time-locked to the onset of the rating
610 (willingness to pay) period with duration of response times (RTs: 1.8 ± 0.5 s). Missed
611 trials were modeled as a separate regressor over the duration of the entire trial. Finally
612 Air-clean trials were modeled separately using three distinct regressors. R10, denoting
613 the instructions period from the Air-clean trials and modeled as a boxcar function time
614 locked at the beginning of the instructions and during 3 seconds. R11, that denoted
615 the stimulus period from the Air-clean trials, starting from the beginning of stimulus
616 (even if the stimulus is a blank odor followed by a dark screen) and during 8 seconds.
617 And R12, that denoted the rating period from the Air-clean trials and modeled as a
618 stick function (because participants didn't have to indicate their willingness to pay).
619 The model also included motion parameters and session constants as regressors of
620 no interest. To test for cognitive regulation, we computed the following contrasts:
621 [Indulge (R5) > Natural (R4)] (Figure 3; *Table 1*), [Distance (R6) > Natural (R4)]
622 (Figure. 4; *Table 1*) at the single level and then used a one-sample t-test at the group
623 level on the single-subject contrast coefficients estimated. We also computed the

624 opposite contrasts at the first level [Natural (R4) > Indulge (R5)] and [Natural (R4) >
625 Distance (R6)] and then similarly used a one-sample t-test at the group level on the
626 single-subject contrast coefficients.

627

628 *Analysis of value computation in the Natural context*

629 We used GLM2 in order to investigate brain regions involved in the computation
630 of value while experiencing food odor and image stimuli. We investigated the brain
631 regions reflecting such value computation by searching for brain areas in which the
632 BOLD response correlated with bids during the Natural trials. GLM2 had one regressor
633 of interest R1, consisting of the values of participants' bids in the Natural trials. The
634 hemodynamic response of this categorical function was convolved with a boxcar
635 beginning at the time of the first odor inspiration and terminating at the bid response
636 (average duration of $10,2 \pm 1.75s$). The instruction period was regressed using a
637 boxcar function, starting from the beginning of instructions with a duration of 3s. GLM2
638 also includes regressors denoting others conditions stimuli (i.e. Indulge and Distance).
639 This regressor consisted of a boxcar function starting from the beginning of inspiration
640 and lasting until the end of rating (average duration of $10.2 \pm 1.78s$). The model also
641 included motion parameters and session constants as regressors of no interest.
642 Finally, Air-clean and missed trials were modeled separately with a duration lasting for
643 the entire trial. In order to reveal brain areas involved in the computation of value,
644 contrasts on the bid parametric modulator on Natural trials were computed. Then, a
645 one-sample t-test was performed at the group level on single-subject contrast
646 coefficients (Figure 5; Table 2).

647 We had strong *a priori* interest concerning the vmPFC and the ventral striatum
648 because previous studies revealed that these regions perform value computation

649 (Hare et al., 2009; Hutcherson et al., 2012; Kober and Mell, 2015; Metereau and
650 Dreher, 2015). Region of Interest (ROI) analysis was thus conducted in a vmPFC ROI
651 defined as an 8-mm diameter sphere, centered at $x,y,z = -2, 40, 2$, based on a previous
652 meta-analysis study showing that this region is involved in the processing of food value
653 presented visually (Clithero and Rangel, 2013), leading to a vmPFC ROI of 573 voxels.
654 Based on this same study, we also defined two ventral striatum ROIs (left VSTR,
655 defined as an 8-mm diameter sphere, centered at $x,y,z = -8, 8, -6$; right VSTR defined
656 as an 8-mm diameter sphere, centered at $x,y,z = 10, 14, -4$, both including 573 voxels.
657 All ROI were defined using WFU_PickAtlas
658 (<http://fmri.wfubmc.edu/software/PickAtlas>). After ROIs creation, they were coregister
659 on the functional images in order to keep voxel size.

660

661 *Analysis of odor preferences encoding*

662 To test for brain regions involved in the subjective preferences of food
663 categories during odor perception, we defined a last GLM, designated GLM3. First of
664 all, because there is no interaction between food category bidding behavior and
665 regulatory conditions, we classified food stimuli categories (i.e. apricot, pineapple, milk
666 chocolate, dark chocolate) from the least preferred to the most preferred, based on
667 the mean bid regardless of the condition for all subjects. This allowed us to classify
668 food categories for twenty-one participants. We were not able to classify food
669 categories for 3 participants because of equal average WTP for at least 2 food
670 categories. This GLM3 is composed of one regressor R1 denoting the instructions
671 period, consisting of a boxcar function starting at the beginning of a trial and lasting 3
672 s. GLM3 also included 4 regressors of interest R2-R5 denoting the least preferred food
673 odor categories (R2), the second less preferred food odor categories (R3), the second

674 most preferred food odor categories (R4) and the most preferred food odor categories
675 (R5). The hemodynamic response was convolved with a boxcar function beginning at
676 the first inspiration at the odor presentation and terminating at the end of the odor
677 presentation(duration 3.2 ± 0.8 s). GLM3 also includes regressors denoting food
678 categories presented visually and ranked similarly to the odor (R6 to R9). The
679 hemodynamic response was convolved with a boxcar function beginning at the picture
680 presentation and lasting for 2 seconds duration. Additionally, the rating period was
681 modeled with a boxcar function starting from the beginning of the rating period and
682 during the entire rating period (1.8 ± 0.61). The model also included motion parameters
683 and session constants as regressors of no interest. To test for brain regions
684 processing individual ranking preferences of food odor categories, we computed the
685 following linear combination: R2, R3, R4 and R5 at the individual level. Then, we used
686 a regression test $R2 < R3 < R4 < R5$ at the group level analysis to identify brain regions
687 encoding individual ranking preferences of odors (Figure 6; Table 3).

688

689 *Functional connectivity between valuation and regulatory regions*

690 A classical study reported that the dlPFC indirectly modulates the vmPFC via
691 the iFG to exert self-control during food choices (Hare et al., 2011). However, a
692 number of subsequent studies did not observe modulation of the vmPFC during
693 cognitive regulation by regulatory regions (Hollmann et al., 2012; Yokum and Stice,
694 2013; Tusche et al., 2018). Here, we tested whether brain regions involved in the
695 valuation of food cues are modulated by regulatory instructions during stimuli
696 perception. To do so, we conducted two ROI-to-ROI generalized Psychophysiological
697 Interaction (gPPI), between regulatory regions (i.e. dmPFC for the Indulge condition
698 and bilateral superior IPFC and right dlPFC for the Distance condition) and valuation

699 regions (vmPFC and bilateral striatum) using the CONN Toolbox
700 (www.nitrc.org/projects/conn, RRID:SCR_009550). This allowed us to explore the
701 changes in connectivity patterns between the regulation and valuation regions
702 according to the regulatory instructions and so, to determine if valuation regions were
703 differentially connected to regulation regions according to the regulatory goals
704 demand. To perform this analysis, preprocessed functional images obtained from SPM
705 as well as the design matrix coming from the GLM1 were loaded into the CONN
706 toolbox. The CONN toolbox implemented the anatomical component-based noise
707 correction method (Behzadi, 2008), extracting principal components related to the
708 segmented CSF and white matter. This approach has been shown to increase the
709 validity, sensitivity and specificity of functional connectivity analyses (Chai et al.,
710 2012). Therefore, white matter and CSF noise components as well as motion
711 parameters (six dimensions with first temporal derivatives resulting in twelve
712 parameters) were regressed out during the denoising step. To control for simple
713 condition-related activation effects, we also included the main task effects (related to
714 GLM1 regressors) as confound regressors during the denoising step.

715 Two gPPI analyses were performed to investigate, in one hand, the difference
716 in functional connectivity between the vmPFC and dmPFC identified with the contrast
717 [Indulge (R5) > Natural (R4)] and, on another hand, the difference in functional
718 connectivity between the vmPFC and the regulation regions identified in the contrast
719 [Distance (R6) > Natural (R4)] with the GLM1. Concerning the Indulge regulation
720 condition, we defined an 8 mm sphere ROI centered on the peak activity (x,y,z:-
721 4,58,21) from the one-sample t-test [Indulge (R5) > Natural (R4)] contrast. For the
722 valuation region, we used the ROI of the vmPFC used for the GLM2 and entered it as
723 target for the first gPPI ROI-to-ROI analysis gPPI-1 (Table 4).

724 For the Distance regulation condition, three others 8-mm diameter sphere ROIs
725 were constructed from the clusters identified in the one-sample t-test [Distance (R6) >
726 Natural (R4)] contrast, centered on the peak activity from the right IPFC, left IPFC and
727 dlPFC (respectively x,y,z: 20,46,30; -24,52,22 and 44,16,46). Here again, the vmPFC
728 ROI from the GLM2 was used as target in this second gPPI ROI-to-ROI analysis gPPI-
729 2 (Table 4).

730 To account for false positives in multiple comparisons, results were thresholded
731 at the peak voxel-level at $p < 0.001$, and then corrected at the cluster-level using a
732 family-wise error rate (FDR) of $p < 0.05$ two-sided.

733

734 **Behavioral analysis**

735

736 Due to excessive head motion, one participant was removed from the fMRI
737 analyses (resulting in $n=24$ for fMRI analysis). Another participant had to be excluded
738 from the leptin/ghrelin Pearson correlation analysis because the hormonal
739 assessment data from this participant was missing (resulting in $n=23$ for this analysis).

740 All statistical analyses were performed using SPSS v21.0 (SPSS Inc., Chicago,
741 IL, USA). Normal distribution was assessed with a Shapiro-Wilk test. If data distribution
742 was not normal, we performed a Friedman test, otherwise a repeated measure
743 ANOVA was conducted. Then, we ensured that homoscedasticity of variances were
744 respected using a Mauchly test. If not, we applied a Greenhouse-Geisser correction
745 to our ANOVA. For multiple comparisons, *post-hoc* (with Bonferroni correction)
746 comparison was conducted according to the previous test used.

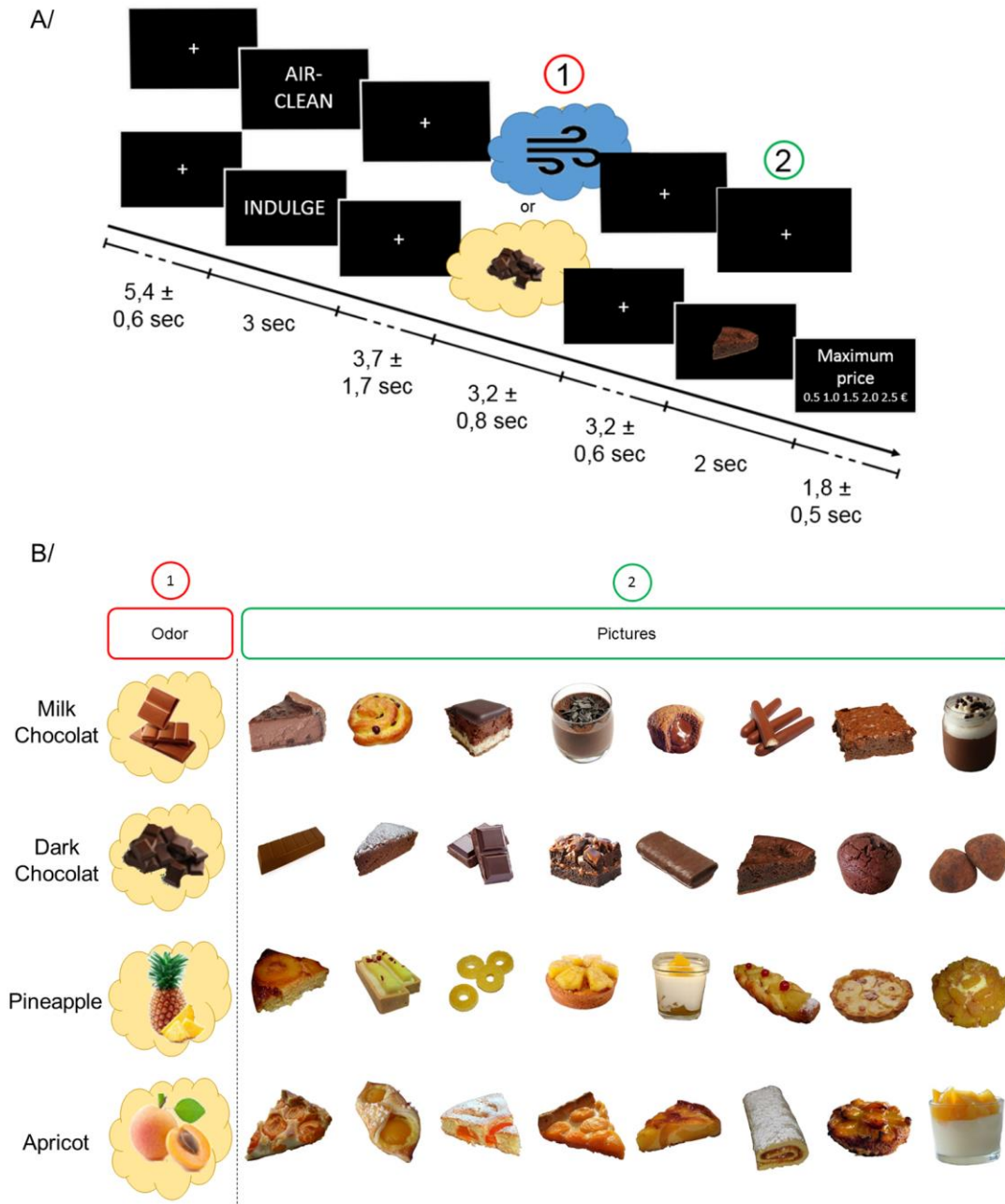
747

748 **Author Contributions**

749 Conceptualization, J.C.D., M. B.; Methodology, J.C.D, R. J., M. F.; Investigation, M.F.,
750 A. F, M.B.; Resources, J.C.D and M.B.; Writing – Original draft, R.J.; M. B. and J.C.D.;
751 Writing – Review & Editing, R.J; E.D. and J.C.D.; Funding Acquisition, J.C.D.;
752 Supervision, J.C.D.

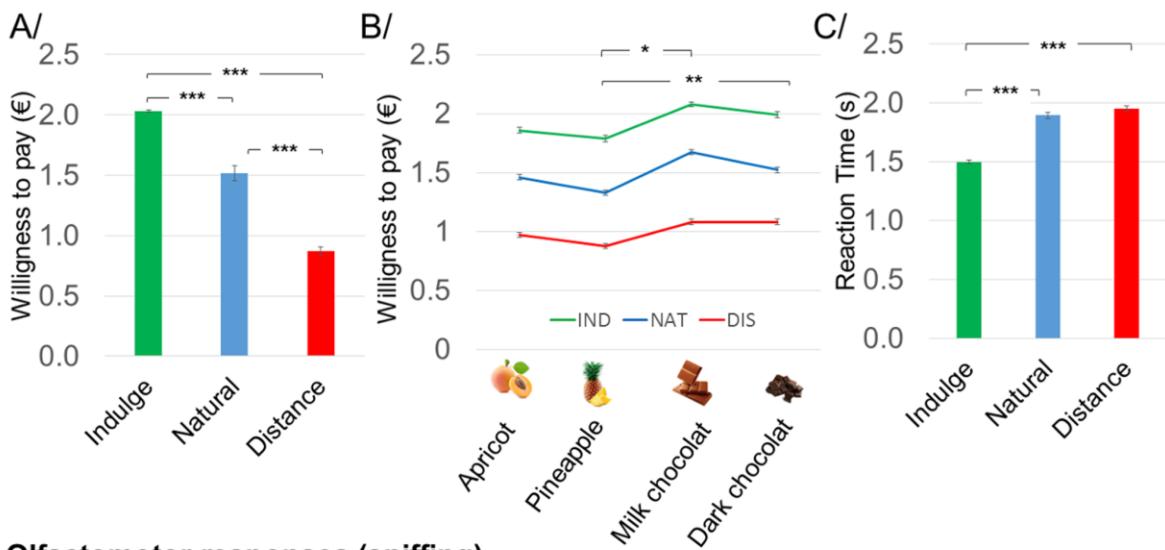
753

754

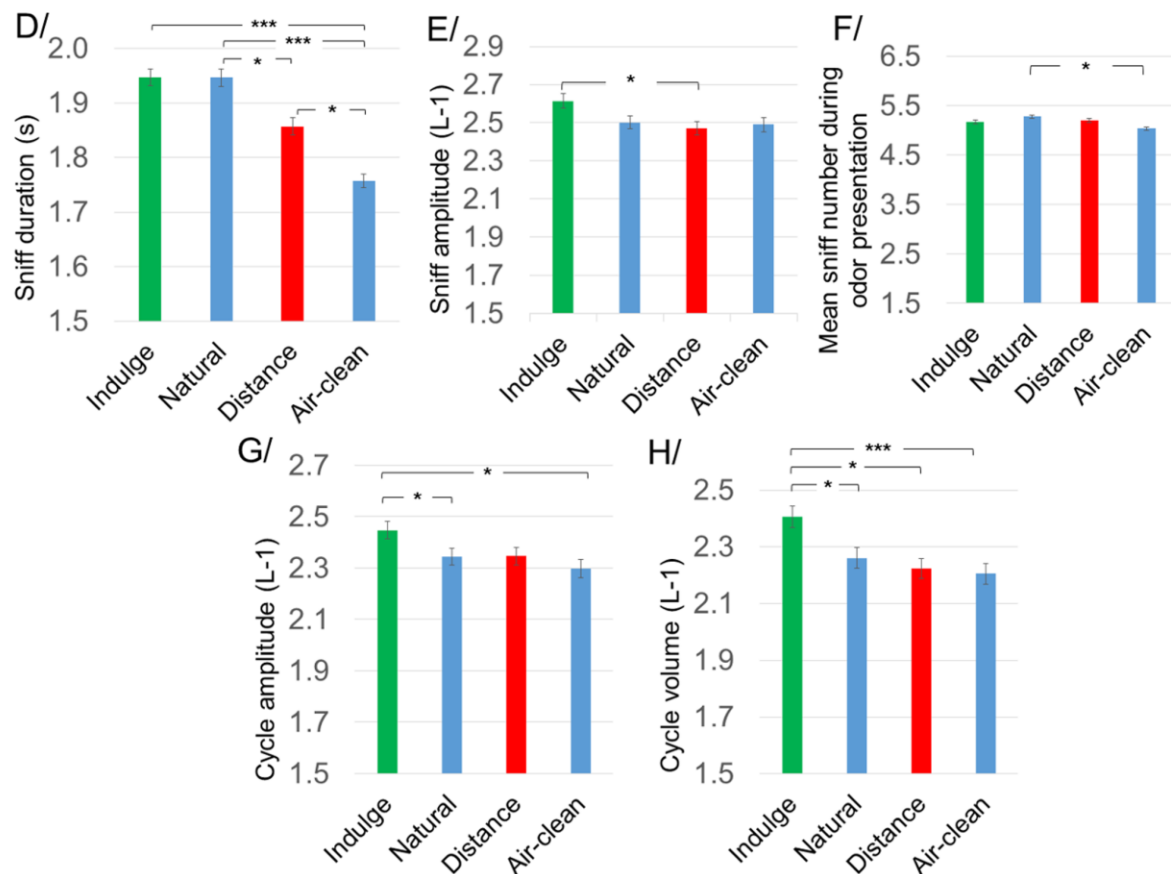


756 **Figure 1: Experimental Design.** (A) Schematic overview of one trial of the task. The
 757 task was composed of four steps. First, hungry participants were given instructions
 758 (Indulge, Natural or Distance) to regulate their craving towards food items. Second,
 759 they smelled one out of four odor categories (Apricot, Pineapple, Milk Chocolate or
 760 Dark Chocolate). Third, a picture of a food item associated to the odor was displayed
 761 (8 food pictures *per* odor category). Finally, participants were asked to rate how much
 762 they wanted to pay to get the food on a 5 points rating scale (from 0.5€ to 2.5€ with
 763 increment steps of 0.5€). (B) Overview of the food items presented. On each trial, a
 764 combination of one odor and one congruent picture (from the same food category)
 765 was presented.
 766

Behavioral response



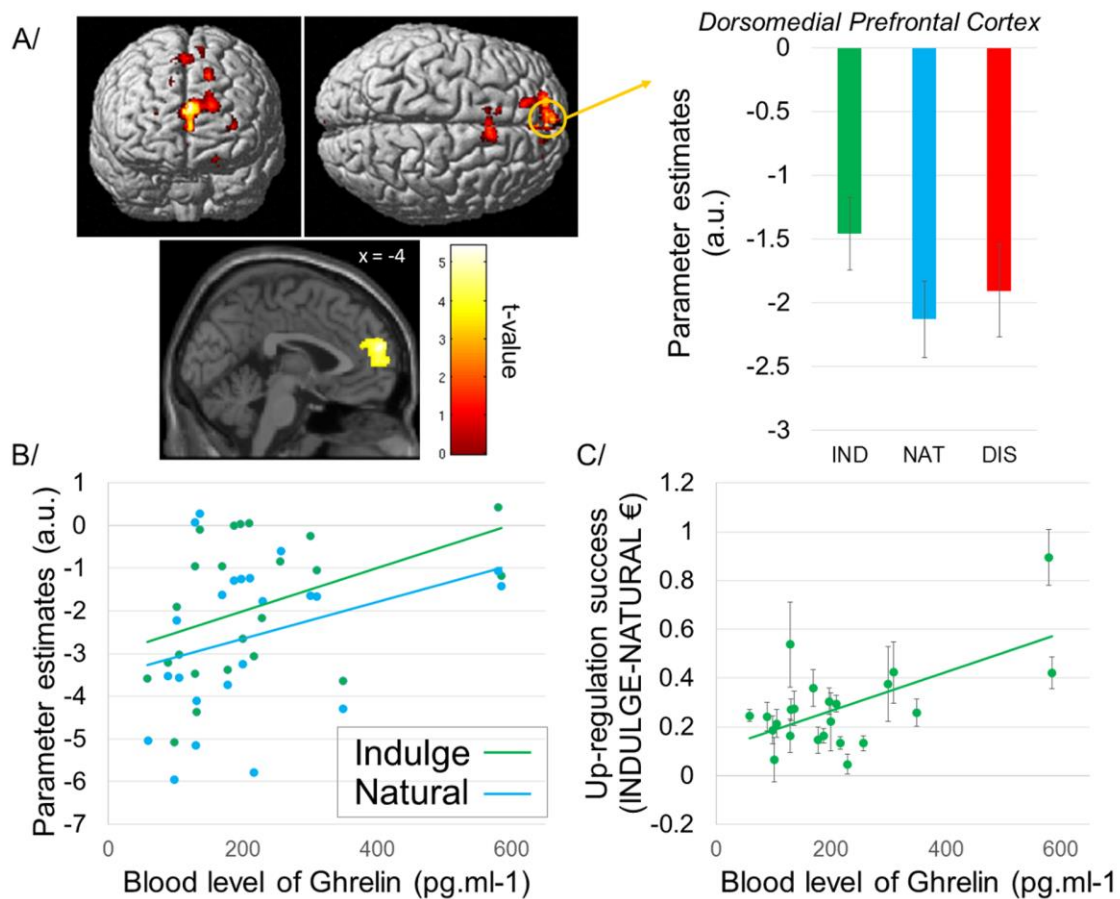
Olfactomotor responses (sniffing)



767

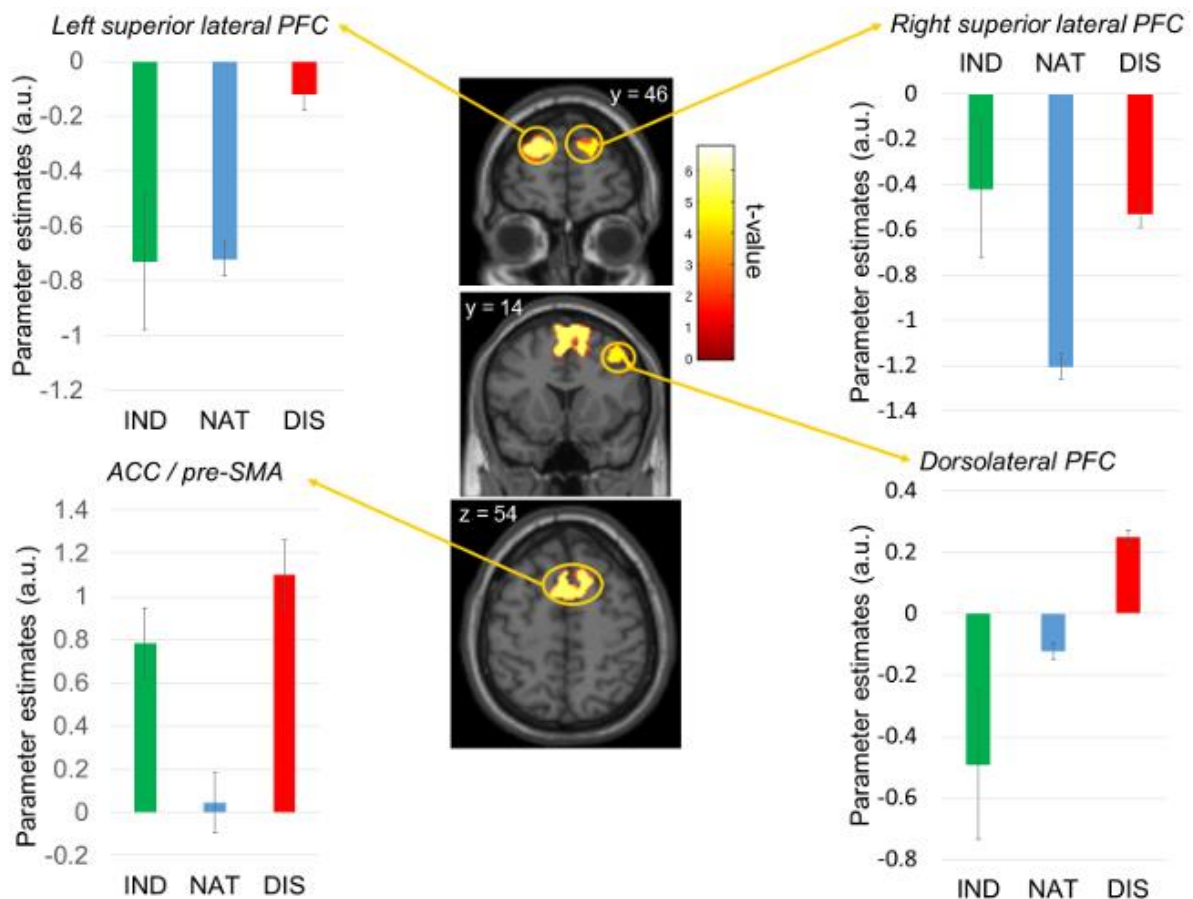
768 **Figure 2: Behavioral and physiological influence of cognitive regulation.** (A)
 769 Average bid across conditions of cognitive regulation. Bids decreased in the Distance
 770 condition compared to Natural, while bids increased in the Indulge condition. (B)
 771 Average bids across conditions and odor categories. Participants were less willing to
 772 pay for pineapple as compared to milk chocolate and dark chocolate. (C) Average
 773 Reaction Times. A decrease in RTs was observed in the Indulge compared to the
 774 Natural and Distance conditions. (D) Average duration of the first sniff. The duration
 775 of the first sniff was shorter in the Distance condition. (E) Average amplitude of the

776 first sniff. The average amplitude of the first sniff was greater in the Indulge condition
777 compared to the Distance condition. (F) Mean number of sniffs during odor
778 presentation. Higher number of sniffs in the Natural compared to Air-Clean trials. (G)
779 Average amplitude of sniffs across the entire period of sniffing. Amplitude was greater
780 in the Indulge condition compared to Natural and Air-Clean conditions. (H) Average
781 volume of sniffs across the entire period of sniffing. Volume was greater in the Indulge
782 condition compared to Natural, Distance and Air-Clean conditions. Error bars show
783 SEM. *** means $p < 0.001$ ** means $p < 0.01$ and * means $p < 0.05$.
784



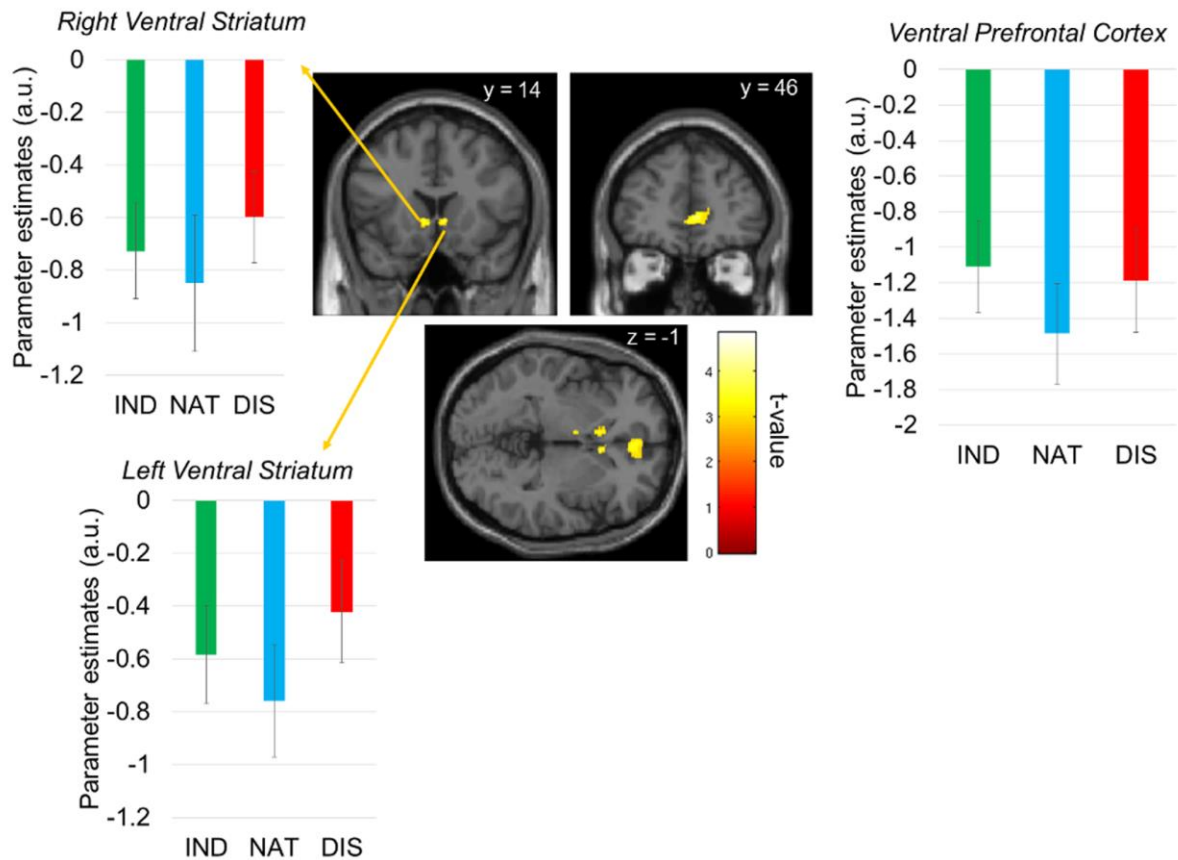
785
786
787
788
789
790
791
792
793
794
795
796
797
798
799

Figure 3: Up-regulation of appetite increases dmPFC activity and inter-individual differences linking up-regulation success and ghrelin levels. (A) Up-regulation during the Indulge condition increased activity in the dorsomedial PFC ($x,y,z: -4, 58, 21$), at a voxel-wise threshold of $p < 0.001$ and cluster size > 40 , corresponding to a whole brain FWE cluster corrected threshold of $p < 0.05$. Error bars show SEM. (B) Positive correlation between blood level of ghrelin and parameter estimates from the Indulge and Natural conditions. Correlation between beta in the Natural condition and ghrelin level $r = 0.469$ ($p = 0.024$) and between beta from the Indulge condition and ghrelin level $r = 0.511$ ($p = 0.013$). (C) Positive correlation between up-regulation success and ghrelin level ($r = 0.373$, $p < 0.05$). Participants showing higher levels of ghrelin were also those showing the higher up regulatory success, as they were willing to pay even more during the Indulge condition.



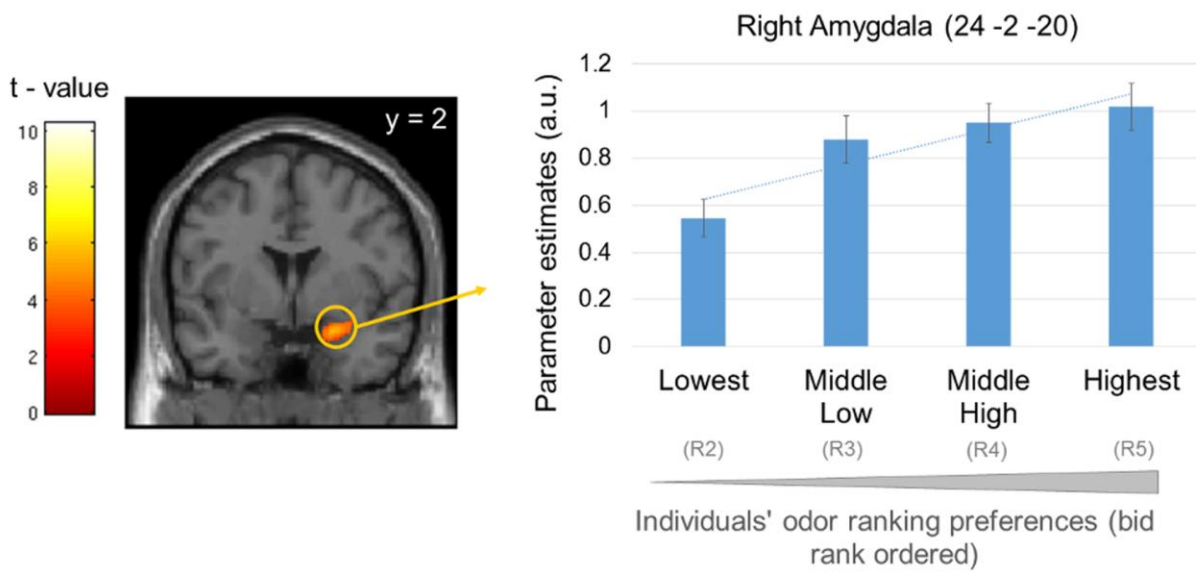
800
801
802
803
804
805
806
807
808
809

Figure 4: Down-regulation during the Distance condition increases activity of the bilateral superior PFC and the right dIPFC. From top to bottom: Left superior lateral PFC (x y z: -24 52 22) and right superior lateral PFC (x,y,z: 20, 46, 30); right dIPFC (x y z: 44 16 46) and ACC/pre-SMA (x,y,z: 3, 8, 62). Graphs indicate beta values extracted from clusters of activity. All activations are reported at a voxel-wise threshold of $p < 0.001$ and cluster size > 40 , which corresponded to a whole brain FWE cluster corrected threshold of $p < 0.05$. Error bars show SEM.



810
 811
 812
 813
 814
 815
 816
 817
 818
 819
 820
 821

Figure 5: vmPFC and bilateral striatum correlate with bids in the Natural condition. The vmPFC (x,y,z: 6, 42, 3) and bilateral striatum (x,y,z: -6, 14, -4 and 6, 18, -2) correlate with the willingness to pay during the Natural condition with no differential effect of the regulation strategies on these regressions. All activations are reported at a whole brain FWE peak corrected threshold of $p < 0.05$. Here the activation map is presented at $p < 0.001$ uncorrected for display. Beta extracted within these regions come from GLM 2. Error bars show SEM.



822

823 **Figure 6: Amygdala activity correlates with individual food category ranking**
 824 **during odor presentation.** *Left.* Right amygdala activity increased with higher
 825 individual ranking (x,y,z: 26, -2, -18). Activations are reported at a whole brain FWE
 826 peak corrected threshold of $p < 0.05$. Similar correlation was observed in the left
 827 amygdala at a lower threshold (x,y,z: -21, 5, -18; $p < 0.005$ uncorrected). Here the
 828 activation map is presented at $p < 0.005$ unc for display purpose only. *Right.* Beta
 829 extracted in right the amygdala for each food category. Error bars show SEM.
 830

Table 1. BOLD changes induced by cognitive regulation

Effect of cognitive regulation during food perception	MNI peak cluster coordinates				
	x	y	z	k	Z score
Indulge > Natural					
Right Superior Medial frontal **	-4	58	21	1505	4.31
Left Superior Medial frontal **	-32	38	12	317	4.01
pre-SMA **	8	16	54	271	3.78
Anterior Cingulate	0	32	-3	75	3.64
Left Superior Medial frontal	-16	45	45	131	3.59
Indulge < Natural					
No brain region					
Distance > Natural					
Left Superior Lateral frontal **	-24	52	22	6343	4.97
Dorsolateral Prefrontal cortex **	44	16	46	561	4.27
Right Angular **	56	-54	27	722	4.22
Left Angular **	-46	-60	39	781	4.13
Right Superior Lateral frontal **	20	46	30	1118	4.03
Distance < Natural					
No brain region					

** cluster reported at $p < 0.05$ FWE whole brain cluster corrected (initial cluster-forming threshold of $p < 0.001$, uncorrected and minimum extent $k = 40$)

832 **Table 1: BOLD changes induced by cognitive regulation during processing of food**
833 **items.** **Clusters are reported at $p < 0.05$, family-wise error (FWE) cluster-level corrected for
834 multiple comparisons (with an initial cluster-forming threshold of $p < 0.001$ and an extent $k =$
835 40 voxels).
836

Table 2. Brain areas correlating parametrically to the bid

	MNI peak cluster coordinates				
	x	y	z	k	Z score
Ventromedial PFC *	6	42	3	1229	3.42
Left Ventral Striatum *	6	18	-2	627	3.19
Right Ventral Striatum *	-6	14	-4	619	3.58
WTP x condition interaction	6	42	3		
No brain region	6	18	-2		

* $p < 0.05$, small-volume corrected within an ROI defined based on literature.

838 **Table 2: Brain areas correlating parametrically to the bid.** ROI analyses were performed
839 using a family wise error (FEW) peak cluster corrected for multiple comparisons. *small
840 volume correction within a sphere ROI of 8 mm centered on peak activity from previous
841 literature (Clithero and Rangel, 2013; Metereau and Dreher, 2015).
842

Table 3. Brain regions correlating to preferences for foods ranked at the individual level

	MNI peak cluster coordinates				
	x	y	z	k	Z score
During odor presentation					
Right Amygdala †	24	-2	-20	348	5.56
Right Occipital **	-24	-96	-12	4429	10.26
Left Occipital **	22	-93	-9	3439	8.01
During picture presentation					
Right Occipital **	-36	-57	-15	48576	23.42
Middle Cingulate cortex **	-6	14	45	3686	13.07
Dorsolateral Prefrontal cortex **	38	6	36	2363	7.19
Right Anterior Insula **	32	30	2	782	6.07
Left Anterior Insula †	-30	26	-4	562	5.92
Right Inferior Parietal cortex †	3	-30	-6	486	4.73
Food preferences x condition interaction (odor)					
No brain region					
Food preferences x condition interaction (picture)					
No brain region					
During odor presentation					

** cluster reported at $p < 0.05$ FWE whole brain cluster corrected (initial cluster-forming threshold of $p < 0.001$, uncorrected and minimum extent $k = 40$)

† peak activity reported at $p < 0.05$ FWE whole brain peak cluster corrected initial cluster-forming threshold of ($p < 0.001$, uncorrected and minimum extent $k = 40$)

843 **Table 3: Brain regions correlating to food ranking preferences for each participant.**
844 **Cluster are reported at $p < 0.05$, family-wise error (FWE) cluster-level corrected for multiple
845 comparisons (with an initial cluster-forming threshold of $p < 0.001$ and an extent $k = 40$
846 voxels). † Cluster are reported at $p < 0.05$, family-wise error (FWE) peak-level corrected for
847 multiple comparisons (with an initial cluster-forming threshold of $p < 0.001$ and an extent $k =$
848 40 voxels).

849

Table 4. Results from the ROI-to-ROI gPPI functional connectivity analyses during stimuli perception.

	Seed	Target ROIs	p-val unc.	p-val FDR	t-value
gPPI - 1 [Indulge>Natural]	dmPFC	vmPFC	0.84	0.96	-0.2
gPPI - 2 [Distance>Natural]	Left IPFC	vmPFC	0.83	0.83	-0,21
	Right IPFC	vmPFC	0.71	0.99	-0.38
	dRight dIPFC	vmPFC	0.83	0.83	-0.21

850

851 **Table 4: Results from the ROI-to-ROI gPPI functional connectivity analysis.** No significant
 852 functional connectivity was identified between regulatory regions and the vmPFC. Initial voxel-
 853 level at $p < 0.005$ for cluster formation, and then corrected at the cluster-level $FDR < 0.05$.

854

855 **References:**

- 856 A.P, Goldstone., C.G., Prechtl., S., Scholtz., A.D. Miras., N. Chhina., G. Durighel., S.S.
857 Deliran., C. Beckmann., M.A. Ghatei., D.R. Ashby., A.D. Waldman., B.D. Gaylinn., M.O.
858 Thorner., G.S. Frost., S.R. Bloom. (2014). Ghrelin mimics fasting to enhance human
859 hedonic, orbitofrontal cortex, and hippocampal responses to food. *Am. J. Clin. Nutr.* 99,
860 1319–1330.
- 861 Abizaid, A., Liu, Z., Andrews, Z.B., Shanabrough, M., Borok, E., Elsworth, J.D., Roth, R.H.,
862 Sleeman, M.W., Picciotto, M.R., Tschöp, M.H., et al. (2006). *Jci0629867.* 116, 3229–3239.
- 863 Adcock, R.A., Thangavel, A., Whitfield-Gabrieli, S., Knutson, B., and Gabrieli, J.D.E. (2006).
864 Reward-Motivated Learning: Mesolimbic Activation Precedes Memory Formation. *Neuron*
865 50, 507–517.
- 866 Anderson, F., Ahluwalia, J.S., Nollen, N.L., and Savage, C.R. (2006). Neural mechanisms
867 underlying food motivation in children and adolescents. *Neuroimage* 27, 669–676.
- 868 Balleine, B.W., and Killcross, S. (2006). Parallel incentive processing: an integrated view of
869 amygdala function. *Trends Neurosci.* 29, 272–279.
- 870 Batterham, R.L., Ffytche, D.H., Rosenthal, J.M., Zelaya, F.O., Barker, G.J., Withers, D.J.,
871 and Williams, S.C.R. (2007). PYY modulation of cortical and hypothalamic brain areas
872 predicts feeding behaviour in humans. *Nature* 450, 106–109.
- 873 Behzadi (2008). A Component Based Noise Correction Method (CompCor) for BOLD and
874 Perfusion Based fMRI. 37, 90–101.
- 875 Billot, P.E., Andrieu, P., Biondi, A., Vieillard, S., Moulin, T., and Millot, J.L. (2017). Cerebral
876 bases of emotion regulation toward odours: A first approach. *Behav. Brain Res.* 317, 37–45.
- 877 Boswell, R.G., Sun, W., Suzuki, S., and Kober, H. (2018). Training in cognitive strategies

878 reduces eating and improves food choice. *Proc. Natl. Acad. Sci.* 115, E11238–E11247.

879 Brooks, S.J., Cedernaes, J., and Schiöth, H.B. (2013). Increased Prefrontal and
880 Parahippocampal Activation with Reduced Dorsolateral Prefrontal and Insular Cortex
881 Activation to Food Images in Obesity: A Meta-Analysis of fMRI Studies. *PLoS One* 8.

882 Buhle, J.T., Silvers, J.A., Wage, T.D., Lopez, R., Onyemekwu, C., Kober, H., Webe, J., and
883 Ochsner, K.N. (2014). Cognitive reappraisal of emotion: A meta-analysis of human
884 neuroimaging studies. *Cereb. Cortex* 24, 2981–2990.

885 Chai, X.J., Castañán, A.N., Öngür, D., and Whitfield-Gabrieli, S. (2012). Anticorrelations in
886 resting state networks without global signal regression. *Neuroimage* 59, 1420–1428.

887 Childress, a R., Hole, a V, Ehrman, R.N., Robbins, S.J., McLellan, a T., and O’Brien, C.P.
888 (1993). Cue reactivity and cue reactivity interventions in drug dependence. *NIDA Res.*
889 *Monogr.* 137, 206–216.

890 Clithero, J.A., and Rangel, A. (2013). Informatic parcellation of the network involved in the
891 computation of subjective value. *Soc. Cogn. Affect. Neurosci.* 9, 1289–1302.

892 Cole, M.W., and Schneider, W. (2007). The cognitive control network: Integrated cortical
893 regions with dissociable functions. *Neuroimage* 37, 343–360.

894 Date, Y. (2013). *Ghrelin and the Vagus Nerve* (Elsevier Inc.).

895 Date, Y., Nakazato, M., and Matsukura, S. (2001). A role for orexins and melanin-
896 concentrating hormone in the central regulation of feeding behavior. *Nippon Rinsho* 59, 427–
897 430.

898 Flegal, K.M., Kruszon-Moran, D., Carroll, M.D., Fryar, C.D., Ogden, C.L., KM, F., KM, F.,
899 KM, F., KM, F., AA, H., et al. (2016). Trends in Obesity Among Adults in the United States,
900 2005 to 2014. *JAMA* 315, 2284.

901 Frank, D.W., Dewitt, M., Hudgens-Haney, M., Schaeffer, D.J., Ball, B.H., Schwarz, N.F.,
902 Hussein, A.A., Smart, L.M., and Sabatinelli, D. (2014). Emotion regulation: Quantitative
903 meta-analysis of functional activation and deactivation. *Neurosci. Biobehav. Rev.* *45*, 202–
904 211.

905 Gallus, S., Lugo, A., Murisic, B., Bosetti, C., Boffetta, P., and La Vecchia, C. (2015).
906 Overweight and obesity in 16 European countries. *Eur. J. Nutr.* *54*, 679–689.

907 Galsworthy-Francis, L., and Allan, S. (2014). Cognitive Behavioural Therapy for anorexia
908 nervosa: A systematic review. *Clin. Psychol. Rev.* *34*, 54–72.

909 Giannopoulou, A., Viergever, M.A., and Smeets, P.A.M. (2018). Effects of hunger state on
910 the brain responses to food cues across the life span. *Neuroimage*.

911 Goldstone, A.P., Thomas, E.L., Brynes, A.E., Castroman, G., Edwards, R., Ghatei, M.A.,
912 Frost, G., Holland, A.J., Grossman, A.B., Korbonits, M., et al. (2004). Elevated fasting
913 plasma ghrelin in Prader-Willi syndrome adults is not solely explained by their reduced
914 visceral adiposity and insulin resistance. *J. Clin. Endocrinol. Metab.* *89*, 1718–1726.

915 Han, J.E., Frasnelli, J., Zeighami, Y., Larcher, K., Boyle, J., McConnell, T., Malik, S., Jones-
916 Gotman, M., and Dagher, A. (2018). Ghrelin Enhances Food Odor Conditioning in Healthy
917 Humans: An fMRI Study. *Cell Rep.* *25*, 2643-2652.e4.

918 Hare, T.A., Camerer, C.F., and Rangel, A. (2009). Self-control in decision-Making involves
919 modulation of the vmPFC valuation system. *Science (80-.)*. *324*, 646–648.

920 Hare, T.A., Malmaud, J., and Rangel, A. (2011). Focusing attention on the health aspects of
921 foods changes value signals in vmPFC and improves dietary choice. *J. Neurosci.* *31*,
922 11077–11087.

923 Holland, P.C., and Gallagher, M. (1999). Amygdala circuitry in attentional and
924 representational processes. *Trends Cogn. Sci.* *3*, 65–73.

925 Hollmann, M., Hellrung, L., Pleger, B., Schlögl, H., Kabisch, S., Stumvoll, M., Villringer, A.,
926 and Horstmann, A. (2012). Neural correlates of the volitional regulation of the desire for food.
927 *Int. J. Obes.* 36, 648–655.

928 Hutcherson, C.A., Plassmann, H., Gross, J.J., and Rangel, A. (2012). Cognitive Regulation
929 during Decision Making Shifts Behavioral Control between Ventromedial and Dorsolateral
930 Prefrontal Value Systems. *J. Neurosci.* 32, 13543–13554.

931 Inui, A., Asakawa, A., Bowers, C.Y., Mantovani, G., Laviano, A., Meguid, M.M., and
932 Fujimiya, M. (2004). Ghrelin, appetite, and gastric motility: the emerging role of the stomach
933 as an endocrine organ. *FASEB J.* 18, 439–456.

934 Inzlicht, M., Berkman, E., and Elkins-Brown, N. (2016). The neuroscience of “ego depletion”:
935 How the brain can help us understand why self-control seems limited. *Soc. Neurosci. Biol.*
936 *Approaches to Soc. Psychol.* 101–123.

937 Jin, J., Zelano, C., Gottfried, J.A., and Mohanty, A. (2015). Human Amygdala Represents the
938 Complete Spectrum of Subjective Valence. *J. Neurosci.* 35, 15145–15156.

939 JM, Z. (2012). Functional Implications of Limited Leptin Receptor and Ghrelin Receptor
940 Coexpression in the Brain. *PLoS One* 32, 736–740.

941 Jones, R.B., McKie, S., Astbury, N., Little, T.J., Tivey, S., Lassman, D.J., McLaughlin, J.,
942 Luckman, S., Williams, S.R., Dockray, G.J., et al. (2012). Functional neuroimaging
943 demonstrates that ghrelin inhibits the central nervous system response to ingested lipid. *Gut*
944 61, 1543–1551.

945 Karra, E., Zelaya, F.O., Rachel, L., Karra, E., Daly, O.G.O., Choudhury, A.I., Yousseif, A.,
946 Millership, S., Iwakura, H., Akamizu, T., et al. (2013). Food-cue responsivity Find the latest
947 version : A link between FTO, ghrelin, and impaired brain food-cue responsivity. *J Clin Invest*
948 123, 3539–3551.

949 Kober, H., and Mell, M.M. (2015). Craving and the Regulation of Craving. Wiley Handb.
950 Cogn. Neurosci. Addict. 5, 195.

951 Kober, H., Mende-Siedlecki, P., Kross, E.F., Weber, J., Mischel, W., Hart, C.L., and
952 Ochsner, K.N. (2010). Prefrontal-striatal pathway underlies cognitive regulation of craving.
953 Proc. Natl. Acad. Sci. U. S. A. 107, 14811–14816.

954 Krishna, A. (2012). An integrative review of sensory marketing: Engaging the senses to
955 affect perception, judgment and behavior. J. Consum. Psychol. 22, 332–351.

956 Kroemer, N.B., Krebs, L., Kobiella, A., Grimm, O., Pilhatsch, M., Bidlingmaier, M.,
957 Zimmermann, U.S., and Smolka, M.N. (2013). Fasting levels of ghrelin covary with the brain
958 response to food pictures. Addict. Biol. 18, 855–862.

959 LaBar, K.S., Gitelman, D.R., Parrish, T.B., Kim, Y.H., Nobre, A.C., and Mesulam, M.M.
960 (2001). Hunger selectively modulates corticolimbic activation to food stimuli in humans.
961 Behav. Neurosci. 115, 493–500.

962 Lebreton, M., Jorge, S., Michel, V., Thirion, B., and Pessiglione, M. (2009). An Automatic
963 Valuation System in the Human Brain: Evidence from Functional Neuroimaging. Neuron 64,
964 431–439.

965 Lewis, G.J., and Bates, T.C. (2014). Neural Systems Underlying the Reappraisal of
966 Personally Craved Foods. Psychologist 26, 194–198.

967 LoMauro, A., and Aliverti, A. (2018). Sex differences in respiratory function. Breathe 14,
968 131–140.

969 Mason, B.L., Wang, Q., and Zigman, J.M. (2013). The Central Nervous System Sites
970 Mediating the Orexigenic Actions of Ghrelin. Annu. Rev. Physiol. 76, 519–533.

971 Metereau, E., and Dreher, J.C. (2015). The medial orbitofrontal cortex encodes a general

972 unsigned value signal during anticipation of both appetitive and aversive events. *Cortex* 63,
973 42–54.

974 Müller, T.D., Nogueiras, R., Andermann, M.L., Andrews, Z.B., Anker, S.D., Argente, J.,
975 Batterham, R.L., Benoit, S.C., Bowers, C.Y., Broglio, F., et al. (2015). *Ghrelin*. 4, 437–460.

976 O’Doherty, J.P. (2004). Reward representations and reward-related learning in the human
977 brain: Insights from neuroimaging. *Curr. Opin. Neurobiol.* 14, 769–776.

978 O’Doherty, J.P., Deichmann, R., Critchley, H.D., and Dolan, R.J. (2002). Neural responses
979 during anticipation of a primary taste reward. *Neuron* 33, 815–826.

980 Ochsner, K.N., and Gross, J.J. (2005). The cognitive control of emotion. *Trends Cogn. Sci.*
981 9, 242–249.

982 Ochsner, K.N., Ray, R.D., Cooper, J.C., Robertson, E.R., Chopra, S., Gabrieli, J.D.E., and
983 Gross, J.J. (2004). For better or for worse: Neural systems supporting the cognitive down-
984 and up-regulation of negative emotion. *Neuroimage* 23, 483–499.

985 Perello, M., and Dickson, S.L. (2015). Ghrelin Signalling on Food Reward: A Salient Link
986 Between the Gut and the Mesolimbic System. *J. Neuroendocrinol.* 27, 424–434.

987 Prescott, J., Burns, J., and Frank, R.A. (2010). Influence of odor hedonics, food-relatedness,
988 and motivational state on human sniffing. *Chemosens. Percept.* 3, 85–90.

989 Saez, R.A., Saez, A., Paton, J.J., Lau, B., and Salzman, C.D. (2017). Distinct Roles for the
990 Amygdala and Orbitofrontal Cortex in Representing the Relative Amount of Expected
991 Reward. *Neuron* 95, 70-77.e3.

992 Seymour, B., and Dolan, R. (2008). Emotion, Decision Making, and the Amygdala. *Neuron*
993 58, 662–671.

994 Sezille, C., Messaoudi, B., Bertrand, A., Joussain, P., Thévenet, M., and Bensafi, M. (2013).

995 A portable experimental apparatus for human olfactory fMRI experiments. *J. Neurosci.*
996 *Methods* 218, 29–38.

997 Shirazi, R., Palsdottir, V., Collander, J., Anesten, F., Vogel, H., Langlet, F., Jaschke, A.,
998 Schurmann, A., Prevot, V., Shao, R., et al. (2013). Glucagon-like peptide 1 receptor induced
999 suppression of food intake, and body weight is mediated by central IL-1 and IL-6. *Proc. Natl.*
1000 *Acad. Sci.* 110, 16199–16204.

1001 Siep, N., Roefs, A., Roebroek, A., Havermans, R., Bonte, M., and Jansen, A. (2012a).
1002 Fighting food temptations: The modulating effects of short-term cognitive reappraisal,
1003 suppression and up-regulation on mesocorticolimbic activity related to appetitive motivation.
1004 *Neuroimage* 60, 213–220.

1005 Siep, N., Roefs, A., Roebroek, A., Havermans, R., Bonte, M., and Jansen, A. (2012b).
1006 Fighting food temptations: The modulating effects of short-term cognitive reappraisal,
1007 suppression and up-regulation on mesocorticolimbic activity related to appetitive motivation.
1008 *Neuroimage* 60, 213–220.

1009 Simmonds, D.J., Pekar, J.J., and Mostofsky, S.H. (2008). Meta-analysis of Go/No-go tasks
1010 demonstrating that fMRI activation associated with response inhibition is task-dependent.
1011 *Neuropsychologia* 46, 224–232.

1012 Sturm, R., Ph, D., and Economist, S. (2013). Morbid Obesity Rates Continue to Rise Rapidly
1013 in the US. 37, 889–891.

1014 Todd A. Hare, Colin F. Camerer, A.R. (2007). Self-Control in Decision-Making Involves
1015 Modulation of the vmPFC Valuation System. *Educ. Technol. Soc.* 10, 257–274.

1016 Tusche, A., and Hutcherson, C.A. (2018). Cognitive regulation alters social and dietary
1017 choice by changing attribute representations in domain-general and domain-specific brain
1018 circuits. *Elife* 7, 1–35.

1019 Uher, R., Murphy, T., Brammer, M.J., Dalglish, T., Phillips, M.L., Ng, V.W., Andrew, C.M.,
1020 Williams, S.C.R., Campbell, I.C., and Treasure, J. (2004). Medial prefrontal cortex activity
1021 associated with symptom provocation in eating disorders. *Am. J. Psychiatry* 161, 1238–
1022 1246.

1023 Wang, G.-J., Volkow, N.D., Telang, F., Jayne, M., Ma, Y., Pradhan, K., Zhu, W., Wong, C.T.,
1024 Thanos, P.K., Geliebter, A., et al. (2009). Evidence of gender differences in the ability to
1025 inhibit brain activation elicited by food stimulation. *Proc. Natl. Acad. Sci. U. S. A.* 106, 1249–
1026 1254.

1027 Wei, X.J., Sun, B., Chen, K., Lv, B., Luo, X., and Yan, J.Q. (2015). Ghrelin signaling in the
1028 ventral tegmental area mediates both reward-based feeding and fasting-induced
1029 hyperphagia on high-fat diet. *Neuroscience* 300, 53–62.

1030 Yokum, S., and Stice, E. (2013). Cognitive regulation of food craving: effects of three
1031 cognitive reappraisal strategies on neural response to palatable foods. *Int. J. Obes. (Lond)*.
1032 37, 1565–1570.

1033 Zanchi, D., Depoorter, A., Egloff, L., Haller, S., Mählmann, L., Lang, U.E., Drewe, J.,
1034 Beglinger, C., Schmidt, A., and Borgwardt, S. (2017). The impact of gut hormones on the
1035 neural circuit of appetite and satiety: A systematic review. *Neurosci. Biobehav. Rev.* 80,
1036 457–475.

1037 Zelano, C., Jiang, H., Zhou, G., Arora, N., Schuele, S., Rosenow, J., and Gottfried, J.A.
1038 (2016). Nasal Respiration Entrain Human Limbic Oscillations and Modulates Cognitive
1039 Function. *J. Neurosci.* 36, 12448–12467.

1040

1041